



Mass balance of nine trace elements in two karst catchments in southwest China

Jicheng Xia^{a,f}, Jianxu Wang^{a,b}, Leiming Zhang^c, Xun Wang^{a,d}, Wei Yuan^a, Hui Zhang^a, Tao Peng^{a,e}, Xinbin Feng^{a,b,*}

^a State Key Laboratory of Environmental Geochemistry, Institute of Geochemistry, Chinese Academy of Sciences, Guiyang 550081, China

^b CAS Centre for Excellence in Quaternary Science and Global Change, Xi'an 710061, China

^c Air Quality Research Division, Science and Technology Branch, Environment and Climate Change Canada, Toronto M3H5T4, Canada

^d College of Resources and Environment, Southwest University, Chongqing 400715, China

^e Puding Karst Ecosystem Research Station, Chinese Academy of Sciences, Puding 562100, China

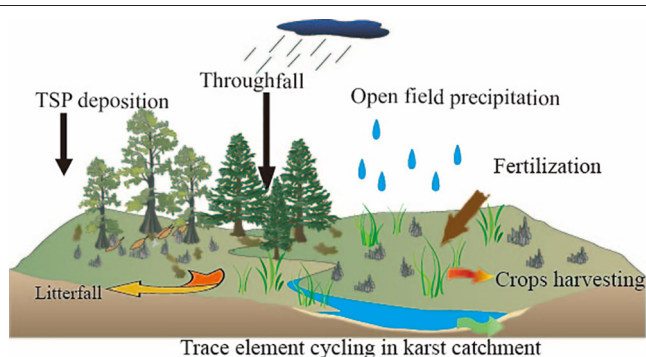
^f University of Chinese Academy of Sciences, Beijing 100049, China



HIGHLIGHTS

- Mass balances of nine TEs in two karst catchments in SW China have been quantified.
- Litterfall and crops dominated the input/output fluxes of TEs in the karst catchment.
- Land use structure played an important role in shaping the fates of the TEs.

GRAPHICAL ABSTRACT



ARTICLE INFO

Article history:

Received 22 March 2021

Received in revised form 27 April 2021

Accepted 29 April 2021

Available online 4 May 2021

Editor: Jay Gan

Keywords:

Trace elements
Karst catchments
Source and sink
Mass balance
Land use types

ABSTRACT

High geological background levels of trace elements (TEs) and high population density in the karst areas of southwest China have imposed environmental pressure on the fragile ecosystems in this region. Understanding the mass budget of TEs, especially the toxic ones, is of great importance to sustain future developments. This study investigates the mass balance and fate of nine TEs (cadmium, arsenic, lead, chromium, copper, nickel, zinc, thallium, and antimony) in two karst catchments (Huilong and Chenqi) in southwest China through estimation of their mass budgets in throughfall, open field precipitation, total suspended particulate matter (TSP), litterfall, fertilization, harvested crops, surface runoff, and underground runoff. The estimated net fluxes are positive, indicating a source region, for four elements (Cu, Cr, Ni, and Tl) and negative, indicating a sink region, for five elements (As, Cd, Pb, Sb, and Zn) in both catchments. The net fluxes for the nine elements in Chenqi catchment are within a relatively small range (2.6, 2.0, 1.6, 0.6, -0.05 , -0.5 , -2.9 , and -3.3 $\text{mg m}^{-2} \text{yr}^{-1}$ for Cu, Ni, Cr, Tl, Cd, Zn, Sb, Pb, and As, respectively), but in Huilong catchment in quite a large range (15.5, 6.0, 1.0, 0.8, -0.3 , -0.9 , -4.5 , -7.5 , and -8.7 $\text{mg m}^{-2} \text{yr}^{-1}$ for Tl, Cr, Ni, Cu, Cd, Sb, As, Pb, and Zn, respectively). Rainfall (12.3%–66.2%) and litterfall (18.4%–81.3%) are the major input flux pathways, while crops harvest (16%–99%) is the major output flux pathway for the TEs in both catchments, indicating that the fate of TEs is shaped by both natural factors such as precipitation and litterfall and human activities such as fertilization and crop harvesting in these forestland-farmland compound karst catchments. Results from this study suggest that restoring forests from low-yield sloping farmlands will be useful for controlling TEs pollution in these fragile karst regions with high geological background TEs.

© 2021 Elsevier B.V. All rights reserved.

* Corresponding author at: State Key Laboratory of Environmental Geochemistry, Institute of Geochemistry, Chinese Academy of Sciences, Guiyang 550081, China.
E-mail address: fengxinbin@vip.skleg.cn (X. Feng).

1. Introduction

Karst rocky desertification refers to the process of soil degradation in the fragile karst environment, and it has occurred in subtropical zones, such as the Mediterranean Basin, the Dinaric karst area, and southwest China (Brinkmann and Parise, 2012; Huang et al., 2008; Jiang et al., 2014; Liu et al., 2019). It is one of the main types of land desertification driven by human activities, and is characterized by degradation of land productivity, resulting in a desert-like appearance of the landscape (Cao et al., 2018; Liu et al., 2020).

China has the largest karst land area in the world. 13.5% of China's land area, or 1.3 million km², belongs to karst landscape. The widest karst landscape in China is the one continuously distributed in southwest China covering an area of 0.62 million km² (Huang et al., 2008). This area has become ecologically fragile due to the high geological background levels of most heavy metals and arsenic, and serious water and soil erosion caused by natural factors and human activities (Li and Jia, 2018; Wu et al., 2020; Xiao et al., 2004a). Intensive farming and mining activities and rapid extension of urban and industrial areas have caused increasing TEs pollution in air, water and soil, which has been documented by long-term measurements of atmospheric deposition, vegetation, soil, and sediments (Su et al., 2008; Weiss et al., 2002; Zheng et al., 2007). Emissions from industrial production, traffic, mining, and agricultural activities have led to the widespread redistribution of TE pollutants among the different environmental media and areas (Huang et al., 2018; Imseng et al., 2019; Lin et al., 2019). The destruction of the karst ecological environment has seriously affected the regional environmental quality and the safety of agricultural products (Fajkovic et al., 2011; Gill et al., 2018).

Extensive disorderly mining and agricultural and industrial activities have caused large loads of toxic TEs (e.g., Cd, As, Pb, Cr, Cu, Ni, Zn, Sb, and Tl) on the fragile ecological systems in regions with high geological background concentrations of TEs (Bi et al., 2006; Sun et al., 2019; Xiao et al., 2019; Xiao et al., 2004a, 2004b). The geochemical behaviour and input/output pathways of TEs in the karst areas remain poorly characterized, limiting our ability to assess the potential impacts of TEs on the sensitive ecosystems and on human health at the regional scales (Ci et al., 2014; Liu et al., 2019). Thus, this study was designed to identify the primary input/output pathways of TEs in two catchments in the karst areas of southwest China and quantify the mass budget of TEs at the catchment scale. The results were also used to determine if these typical karst catchments are sinks or sources of TEs. Such knowledge is needed for the prevention and control of TE pollution in these fragile karst regions.

2. Materials and methods

2.1. Sites description

The two karst catchments (Huילong and Chenqi) previously selected for investigating mercury mass balance were also selected in this study for investigating TEs mass balance (Xia et al., 2021). Huילong catchment (18 ha) is located in the southwest part of Guizhou province, and Chenqi catchment (150 ha) is located in the central part of the same province (Fig. S1). The two catchments, Huילong and Chenqi, were evolved from detrital sandstone and limestone, respectively (Sun et al., 2012; Zhao et al., 2010). There was metal mining activity before 1950s in Huילong, but there are no proven metal deposits in Chenqi. These two catchments are representative of this region, with the former having high and the latter having low geological background levels of TEs. The land use across the two catchments were calculated using Arc GIS 10.4. About 17% and 20% of the catchment area were used for agricultural production in Huילong and Chenqi, respectively, and forestry accounts for most of the remaining land use. Special considerations were given to the characteristics of the topography

and geomorphology of both catchments when selecting the sampling sites so that the two catchments were relatively closed with a clear boundary. More information about these two catchments can be found in Xia et al. (2021).

2.2. Sampling and chemical analysis

The layout of the sampling points and the sample collection methods are basically the same as those described for the mercury mass balance study presented in Xia et al. (2021), but different chemical analysis methods were used in this study.

2.2.1. Open field precipitation and throughfall sampling

Monthly open field precipitation and throughfall samples were collected at open sites and inside forests, respectively, from August 2018 to July 2019. One open field precipitation sampling site was set up in each of the catchments. Two and three throughfall sampling sites were setup in the Chenqi and Huילong catchments, respectively. The open field precipitation and throughfall samples were acidified using 1% ultra-pure HNO₃, stored in a 4 °C refrigerator, and analysed within one week of their collection.

2.2.2. Runoff sampling

The surface runoff and underground runoff in the two catchments were sampled monthly from August 2018 to July 2019. The pre-treatment method was similar to that used for the rainwater samples. Annual mean air temperature was 15.2 °C and 15.1 °C, and annual mean precipitation amount was 1315 mm and 1378 mm in Huילong and Chenqi, respectively (Xia et al., 2021). Rainfall was mainly concentrated in May to October. Due to the abundant ground seams in the karst areas, a large amount of surface runoff entered the ground along the ground seams.

2.2.3. TSP sampling

The total suspended particulate matter (TSP) was sampled monthly from August 2018 to July 2019, with each sample covering a 48-hour collection period. TSP was collected using a TSP sampler (gas flow rate 100 l min⁻¹, KB-120F, Qingdao jingcheng instrument co. LTD) with a ϕ 90 mm quartz filter film (Munktell Inc. Sweden) for TEs concentration analysis. In order to calculate the deposition flux of TEs through TSP, the deposition velocity of TSP is needed. For this purpose, TSP was also simultaneously collected using a TSP collecting cylinder (30-cm high, 15-cm diameter, Taiheng plastics co. LTD; 100 ml of pure water and 50 ml of ethylene glycol were added), and the deposition velocity of TSP was calculated from the collected mass of TSP by cylinder and the sampling time (see Fig. S5).

2.2.4. Fertilizer sampling

Chemical fertilizer samples and livestock manure samples were collected from farms near Huילong and Chenqi villages.

2.2.5. Litterfall sampling

Fifteen and seven litterfall boxes (1-m side length) were installed 0.3 m above the ground in the Huילong and Chenqi catchments, respectively. The litterfall was sampled monthly from August 2018 to July 2019. Three monthly samples were mixed together to obtain a combined sample for each box. The samples were air-dried, ground, and homogenized before analysis.

2.2.6. Crops sampling

The crops were sampled every three months from August 2018 to July 2019. The collected crops include corn, rice, vegetables, etc. (Table S4). The sampling method was referred to the one used by local farmers for harvesting crops. The edible parts and straw were collected respectively.

2.2.7. Soil sampling

According to the different land use types (forestland and farmland) and the different altitudes, 11 and 23 surface soil samples were collected in the Huilong and Chenqi catchments, respectively, and 15 cm depth of surface soil were collected using a soil sampler. The GPS coordinates were recorded. The samples were placed in numbered sample bags, brought back to the laboratory, dried at 40 °C by oven, and then measured the dry sample weight. The visible plant tissue, stones, and other debris were removed from the soil samples. Each soil sample was crushed into 200-mesh, packed, and recorded for further chemical analysis.

2.2.8. Chemical analysis

TEs concentrations in the open field precipitation, throughfall, surface runoff, underground runoff, TSP membrane filter, fertilizer, litterfall, crop, and soil samples were analysed using inductively coupled plasma mass spectrometry (ICP-MS, refer to the USA Environmental Protection Agency's Method 6020B). The water samples were filtered through a 0.45- μm membrane filter (MFS, cellulose acetate, $\varphi = 47$ mm). Subsamples of water were transferred into carefully cleansed PTFE bottles, acidified with 2% sub-boiling distilled HNO_3 , and preserved at 4 °C.

The filter samples were stored at -18 °C before being freeze dried using a lyophilizer (EYELA FDU-2110, Tokyo Physical and Chemical Equipment Co., Ltd.) operated at -80 °C and 3 Pa for 72 h. The plant samples were digested in sub-boiling distilled HNO_3 . The filter membrane and other solid samples were digested using a mixture of sub-boiling distilled HNO_3 and HF.

The general steps used for chemical analysis are as follows. About 0.1 g of sample was weighed into a Teflon digestion tank, 5 ml of double-distilled ultrapure HNO_3 and 1 ml of double-distilled HF were added in sequence, and the Teflon inner cup was placed in the steel jar. The steel jar was tightened, placed in an oven, and heated at 150 °C for 48 h. In a fume hood, 1 ml of 30% H_2O_2 was added into the Teflon inner cup. The Teflon cup was placed on a hotplate, and the acid was evaporated at 90 °C until the sample was nearly dry. It was then transferred to a centrifuge tube (BIOFIL®) and diluted to 10 ml for testing.

2.3. Mass of environmental media and land use data

The rainfall, surface runoff, and underground runoff data in the Chenqi catchment were provided by the Puding Karst Ecosystem Research Station, Chinese Academy of Sciences (CAS). The rainfall depth in the Huilong catchment was measured using a rain bucket ($\varphi = 200$ mm, TZTZ Co., Ltd.). The surface runoff and underground runoff depths in the Huilong catchment were measured using a Parshall flume (Green Co., Ltd.). The annual mass of fertilizer was determined by consulting with the local farmers. The annual mass of the litterfall or crops was calculated through multiplying the weight of the sample per unit area in the sample square by the area of forest or farmland. The land use area was calculated using Arc GIS 10.4, with the original data source of different land use areas being acquired by using a handheld GSP locator (Zhuolin Co., Ltd.).

2.4. QA/QC and statistical analysis

Reference materials soil GBW07405 and plant GBW10014 were used for the quality control (QC). The recoveries of the matrix spikes ranged from 89% to 110%. Five milli-Q water blanks were setup during the sampling and digestion period. The blanks were measured throughout the study and were all below the detection limits of the measured TEs. The relative percentage difference of the sample replicates was <5%.

Five input pathways and three output pathways of TE transportation in the two karst catchments were investigated. The input pathways include throughfall, open field precipitation, litterfall, TSP, and

fertilization. The output pathways include crops harvesting, surface runoff, and underground runoff. The TE transport fluxes through the two catchments were calculated by multiplying the TE concentrations by the rainfall/runoff depth (mm yr^{-1}), yield ($\text{kg ha}^{-1} \text{yr}^{-1}$), or deposition rate (cm s^{-1}). The calculation of the eight pathways is described as follows:

$$F = \sum_{i=1}^m \sum_{j=1}^n C_{ij} \times E_{ij} \times K_i \quad (1)$$

where F ($\text{mg m}^{-2} \text{yr}^{-1}$) is the annual mass flux of the TEs; C ($\mu\text{g L}^{-1}$, $\mu\text{g g}^{-1}$, or ng m^{-3}) is the annual TE concentration; E (mm yr^{-1} , $\text{kg ha}^{-1} \text{yr}^{-1}$, or cm s^{-1}) is the annual exported volume per year or mass per year; K is the unit conversion factor; i represents the different pathways; and j represents the different catchments.

The mercury mass balance equation that was first described in Feng et al. (2009) and was later used by Xia et al. (2021) was used here to investigate TEs mass balance. The net flux of this equation can be an indicator of whether a particular study area is a source or sink of a potentially toxic element (Gao et al., 2006; Macleod et al., 2005). The equation is described as follows:

$$\text{Net flux} = \sum \text{output flux} - \sum \text{input flux} \quad (2)$$

where $\sum \text{input flux}$ and $\sum \text{output flux}$ are the annual total of the TE fluxes from the input and output pathways, respectively, at the catchment scale.

3. Results

3.1. TEs in throughfall, open field precipitation, surface runoff, and underground runoff

TEs distributed in the various types of water samples (throughfall, open field precipitation, surface runoff, and underground runoff) in Huilong and Chenqi catchments are shown in Fig. 1. In Huilong catchment, annual average concentrations of the nine TEs, in sequence of lowest to highest, were 0.24, 0.37, 0.95, 3.10, 3.28, 3.28, 3.63, 4.18, and 27.6 $\mu\text{g L}^{-1}$ for Tl, Cd, Sb, Cu, Pb, Cr, Ni, As, and Zn, respectively, in the throughfall (TF), 0.15, 0.30, 0.66, 1.87, 2.05, 2.07, 2.49, 2.58, and 23.2 $\mu\text{g L}^{-1}$ for Tl, Cd, Sb, Pb, Ni, Cu, Cr, As, and Zn, respectively, in the open field precipitation (OP), 0.12, 0.23, 0.34, 0.58, 0.68, 1.20, 1.65, 1.85, and 6.01 $\mu\text{g L}^{-1}$ for Sb, Cd, Tl, Ni, Pb, As, Cu, Cr, and Zn, respectively, in the surface runoff (SR), and 0.08, 0.09, 0.11, 0.21, 0.74, 1.00, 1.16, 2.33, and 7.37 $\mu\text{g L}^{-1}$ for Tl, Cd, Sb, Pb, Ni, As, Cu, Cr, and Zn, respectively, in the underground runoff (UR). The distribution trends of the TEs in Chenqi catchment were very similar to those in Huilong catchment shown above, although the concentrations of most of the TEs in the environmental media discussed above were somewhat lower in Chenqi than Huilong.

For all of the TEs, annual concentrations in the throughfall were 19.2%–77.1% higher than those in the open field precipitation in Huilong catchment. The concentration in the surface runoff were actually 6.6%–96.2% lower than those in the open field precipitation for all the TEs except Tl. The concentrations of Zn were much higher than the rest of the TEs in all of the four types of water samples. As, Cr, and Cu had relatively higher concentrations than the other TEs.

The seasonal patterns of the TEs concentrations were also examined by splitting the year into dry (Nov–Apr) and wet (May–Oct) seasons. The concentrations of the TEs in the open field precipitation and throughfall (Fig. S7) were both higher in the dry than wet season in Huilong catchment (by 0.52–9.52 times, $p < 0.05$) and Chenqi catchment (by 0.39–10.62 times, $p < 0.05$). There were no apparent seasonal variations in the concentrations in the surface and ground runoff.

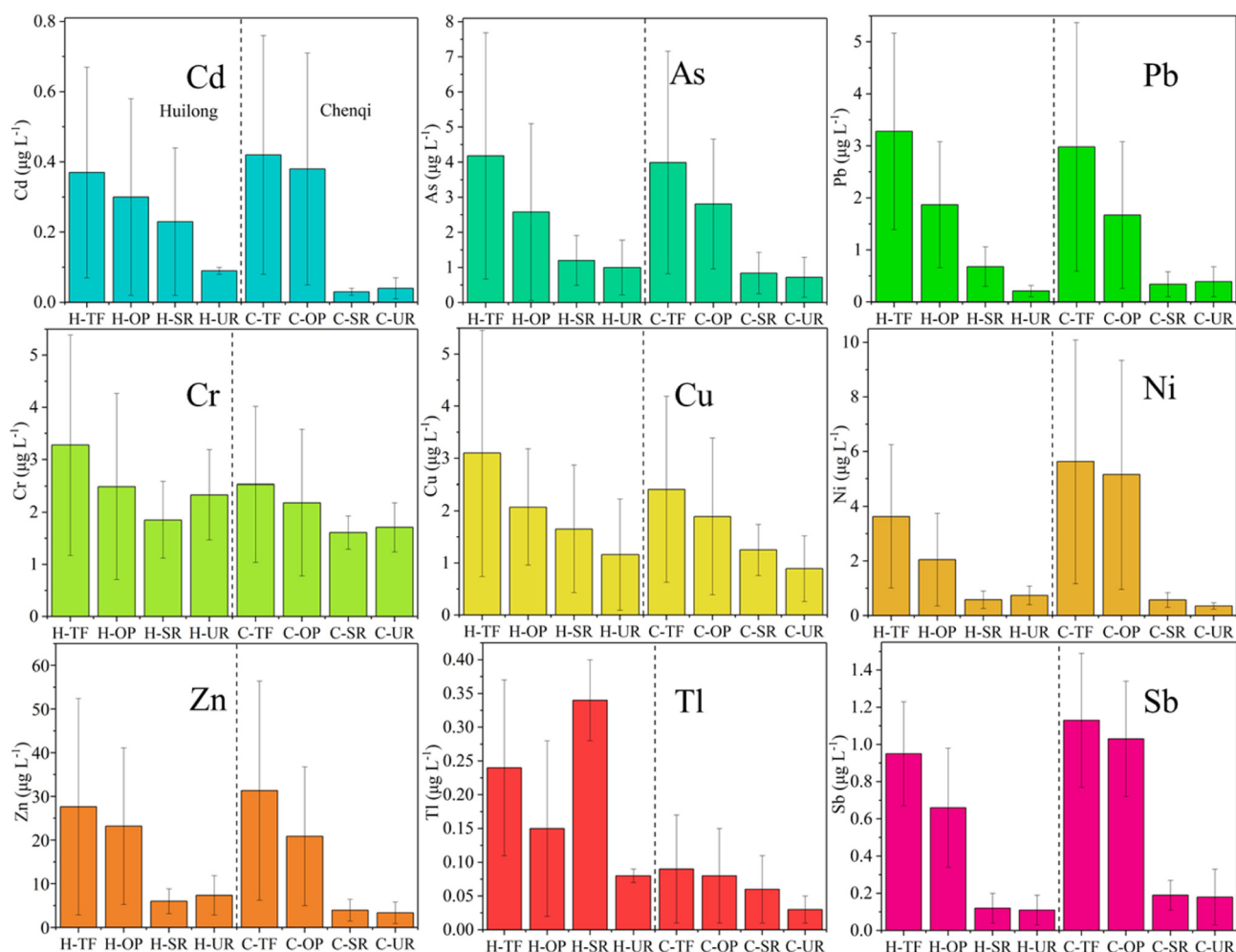


Fig. 1. Annual average TE concentrations in throughfall (TF), open field precipitation (OP), surface runoff (SR), and underground runoff (UR) in Huilong catchment (H-TF, H-OP, H-SR, and H-UR) and the Chenqi catchment (C-TF, C-OP, C-SR, and C-UR). The differences in the TE concentrations of the water samples in the Huilong and Chenqi catchments were significant at $p < 0.05$. The error bars denote standard deviation (1SD) from the mean. The detailed data are presented in Table S1 in the Supplementary Information (SI).

3.2. TEs in TSP and litterfall

In Huilong catchment, annual average concentrations of the TEs, in sequence of lowest to highest, were 0.40, 0.60, 0.74, 1.31, 2.45, 4.60, 15.1, 18.9, and 27.5 ng m^{-3} for Cd, Tl, Sb, Ni, Cr, Cu, As, Pb, and Zn, respectively, in TSP, and 0.46, 0.47, 1.41, 1.50, 3.18, 5.92, 8.58, 10.3, and 77.4 $\mu\text{g g}^{-1}$ for Sb, Cd, Tl, As, Cr, Ni, Pb, Cu, and Zn, respectively, in litterfall. The distribution trends of the TEs in Chenqi catchment were similar to those in Huilong catchment. TE concentrations in TSP were higher by 0.21–3.01 times ($p < 0.05$) in Huilong than Chenqi catchment. Tl concentrations in LF were higher by 27.2 times while those of the other TEs by up to 2.4 in Huilong than Chenqi catchment (Fig. 2).

The seasonal variations in TEs concentrations in TSP were significant ($p < 0.05$) in Huilong catchment, with concentrations being higher by 0.32–0.93 times in dry than wet season. Similar seasonal trends were also observed in Chenqi catchment with concentrations being 0.04–2.79 times higher in dry than wet season.

3.3. TEs in fertilizers and crops

As shown in Fig. 3, the nine TEs concentrations were higher by 0.18–13.6 times ($p < 0.05$) in livestock manure than chemical fertilizers in Huilong catchment. In Chenqi catchment, concentrations of Ni, Pb, Tl, Cu, and Cd were higher by 0.42–3.55 times ($p < 0.05$) in livestock manure than chemical fertilizers, while those of As, Cr, Zn, and Sb were higher by 0.95–29.1 times ($p < 0.05$) in chemical fertilizers than

livestock manure. Apparently, the choice of fertilizers has important implications for the input of TEs. The amounts of livestock manure and chemical fertilizers used in Huilong were 1500 and 900 kg ha^{-1} , while those in Chenqi were 1200 and 750 kg ha^{-1} , respectively. The amount of livestock manure used in the farmlands was about 1.6 times of that of chemical fertilizers in the two catchments.

The TEs concentrations in the various parts of crops (on dry weight basis) are presented in Fig. 3. Different crops or different parts of the same crop have different capacities for accumulating TEs. In Huilong catchment, TEs concentrations were much higher in the leaves than in the seeds of the coix and corn. The top elements that accumulated in coix leaves were Cu, Tl, and Zn (17.9–24.1 $\mu\text{g g}^{-1}$), in corn leaves were Cr, Cu, Zn (4.6–24.5 $\mu\text{g g}^{-1}$), and in vegetables were Cr, Tl, and Zn (10.4–42.8 $\mu\text{g g}^{-1}$). In Chenqi catchment, TEs concentrations were much higher in leaves than seed for cereal crop. The top elements accumulated in rice leaves were Cu, Cr, Zn (4.0–28.8 $\mu\text{g g}^{-1}$), and in vegetables were As, Cr, Cu, Ni, Zn, Tl, and Sb. The concentrations of some TEs in crops were quite different between the two catchments. For example, Tl concentration in vegetables was 1450 times higher in Huilong than Chenqi.

3.4. TEs in the soil

TEs concentrations in soil should reflect historical bedrock weathering and anthropogenic inputs (Bini et al., 2011; Peng et al., 2014). The concentrations of the nine elements in the soil varied

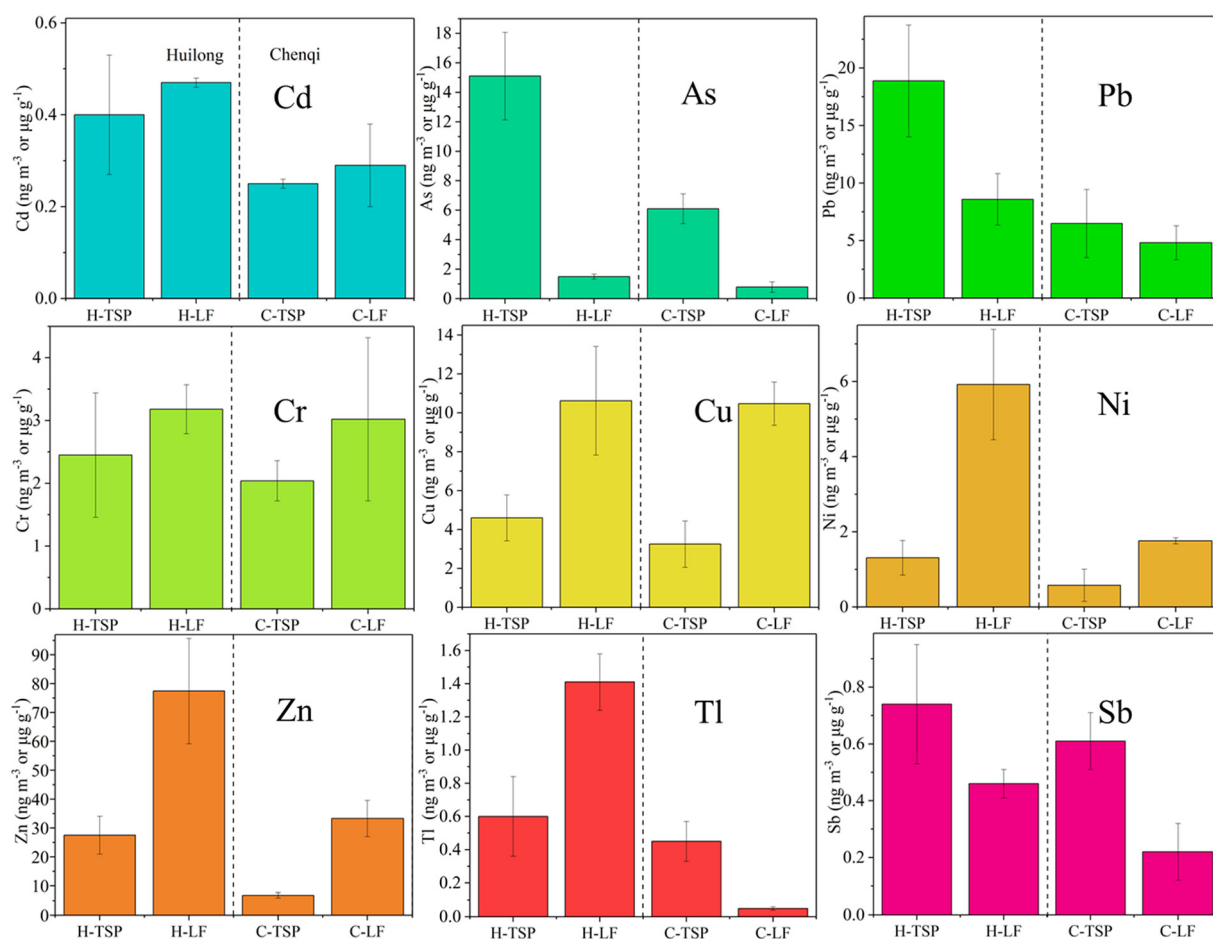


Fig. 2. Annual TE concentrations in TSP (ng m^{-3}) and litterfall ($\mu\text{g g}^{-1}$) in Huilong catchment (H-TSP and H-LF) and Chenqi catchment (C-TSP and C-LF). The differences in the TE concentrations in TSP and LF between Huilong and Chenqi catchments were significant at $p < 0.05$. The error bars denote the standard deviation (1SD) from the mean. The detailed data are presented in Table S1 in the SI.

significantly. The mean Cd and Sb concentrations were in the range of $0.26\text{--}1.75 \mu\text{g g}^{-1}$ while the other seven elements were in the range of $8.3\text{--}128.8 \mu\text{g g}^{-1}$ in Huilong catchment. The mean Cd, Tl, and Sb concentrations were in the range of $0.36\text{--}1.11 \mu\text{g g}^{-1}$ while the other six elements were in the range of $14.0\text{--}61.0 \mu\text{g g}^{-1}$ in Chenqi catchment (Fig. 4).

The background soil concentrations of As, Cr, Cu, Ni, Zn, Tl, and Sb in Huilong catchment were 0.3–13.3 times higher than the background values of the Guizhou soil (Table S3). In contrast, the background soil concentrations of Cd, As, Pb, Cr, Cu, Ni, Zn, Tl, and Sb in Chenqi catchment were all lower than the background values of the Guizhou soil, but those of Cd, As, Pb, Cu, and Ni in Chenqi were 0.08–2.7 times higher than the background values of the Chinese soil.

3.5. TEs mass balance in the two catchments

The net flux for each individual TE in each of the two catchments was calculated using Eqs. (1) and (2). The net fluxes for Cd, As, Pb, Zn, and Sb were negative in Huilong (-0.26 to $-8.75 \text{ mg m}^{-2} \text{ yr}^{-1}$) and Chenqi (-0.05 to $-3.32 \text{ mg m}^{-2} \text{ yr}^{-1}$) catchment, indicating that the two studied catchments were sinks of these elements. The net fluxes of these elements were several times higher in Huilong than Chenqi. The net fluxes for Cr, Cu, Ni, and Tl were positive in Huilong ($0.82\text{--}15.52 \text{ mg m}^{-2} \text{ yr}^{-1}$) and Chenqi ($0.60\text{--}2.65 \text{ mg m}^{-2} \text{ yr}^{-1}$) catchment, indicating that the catchments were sources of these elements (Fig. 5). The net fluxes of Cr and Tl were higher while those of Cu and Ni were lower in Huilong than Chenqi.

4. Discussion

4.1. Characteristics of TEs in the environmental media

The lower TEs concentrations in rainwater in wet than dry season should be mainly caused by the frequent rainfall in the wet season, which washed out frequently TEs in the atmosphere and forest canopy and thus resulted in low TEs concentrations in rainwater in any single rainfall event. The higher TEs concentrations in throughfall than open-field rainwater was apparently due to washing out the additional TEs originally attached to canopy surface by the penetrating rain that ended up as throughfall. The smaller seasonal variations of TEs concentrations in runoff than rainwater was likely due to soil and canopy buffering processes, through which a portion of the TEs mass was intercepted before reaching to runoff. For example, the significantly higher concentrations of Cd, Pb, Zn, and Sb in rainfall than surface runoff and underground runoff indicated large portions of these TEs mass in rainwater being trapped by underlying surfaces. One exception is the case of Tl in Huilong catchment, where significantly higher concentrations were observed in surface runoff than rainfall and underground runoff, which was likely related to the high background soil Tl concentration (e.g., $1.5\text{--}109 \text{ mg kg}^{-1}$) in this catchment. The seasonal variations in TE concentrations of the TSP may be attributed to the fact that the rainfall was more frequent in the wet season and the rainfall had an elution effect on the atmospheric TSP, thereby reducing the concentrations of the particulate-bound TEs in the atmosphere (Mamun et al., 2019). Overall, the seasonal changes in the TE concentrations of the

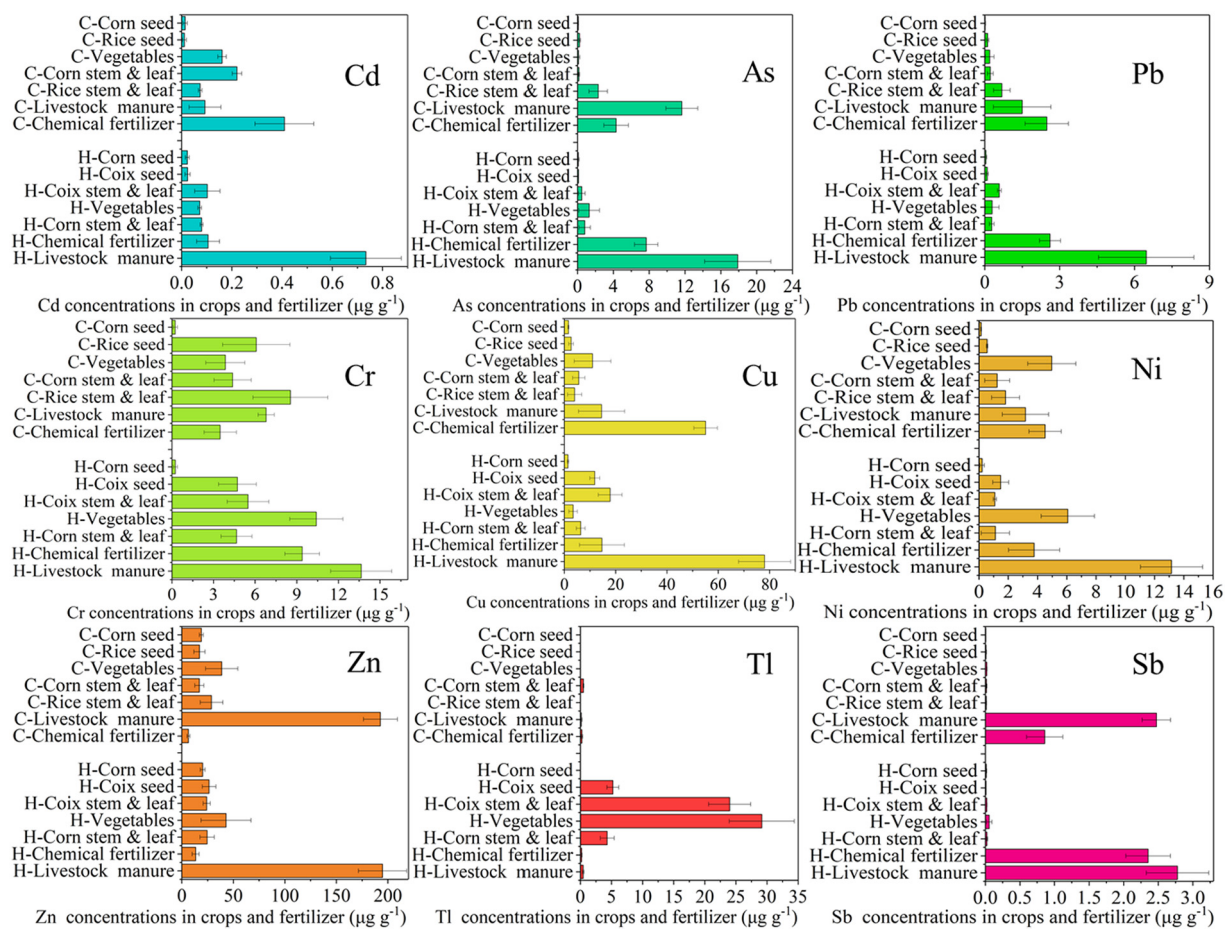


Fig. 3. TEs concentrations in crops and fertilizers in Huilong (denoted as H-) and Chenqi (C-) catchment. The error bars denote the standard deviation (1SD) of the mean.

litter were weak, which may be due to the fact that the leaves experience similar life cycles, and the levels of the accumulated TEs were closer (Aničić et al., 2011; Censi et al., 2017).

Since Huilong is located in a remote area and Chenqi in a suburb area, based on the distribution of the soil TE concentrations, it is speculated that, while the high TE concentrations in TSP in Huilong were mainly caused by the high geological background TE concentrations, TEs in TSP in Chenqi were mainly originated from crustal dust and industrial emissions into the atmosphere. TEs concentrations in litterfall were higher in Huilong than Chenqi, consistent with the trend of TEs

in TSP since atmospheric TSP can be effectively captured by vegetation (Luo et al., 2019).

The higher TE concentrations in crops in Huilong than Chenqi were caused by the combined effects of higher atmospheric deposition and higher background soil TEs in Huilong, resulting in higher risks of TEs exposure to local residents in Huilong from consumption of local agricultural products. Since crop straw was mainly recycled as animal feed, extensive farming activities led to constant cycling of TEs between the soil, crops, and livestock manure (Bolan et al., 2004; Xia et al., 2017).

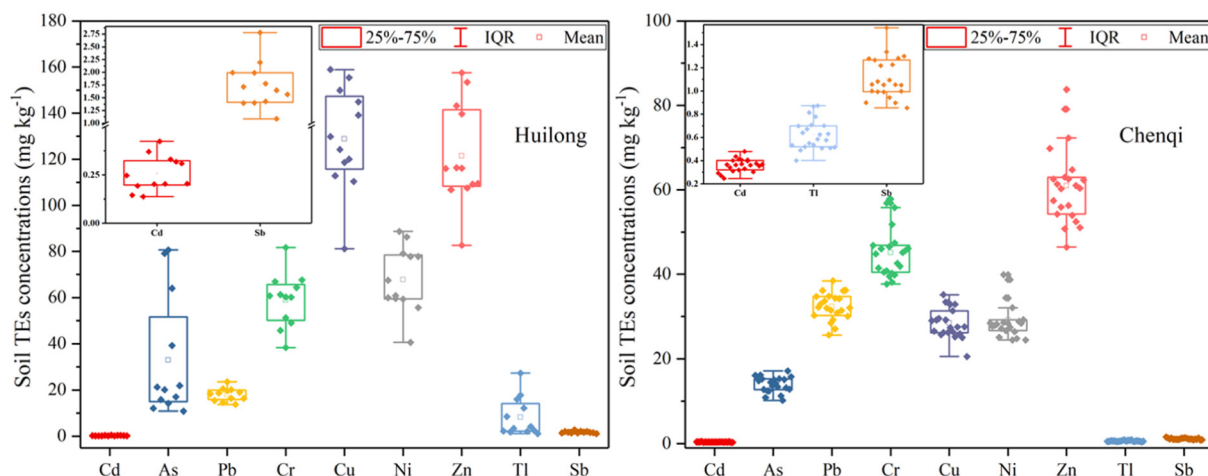


Fig. 4. Soil TEs concentrations in Huilong and Chenqi catchments.

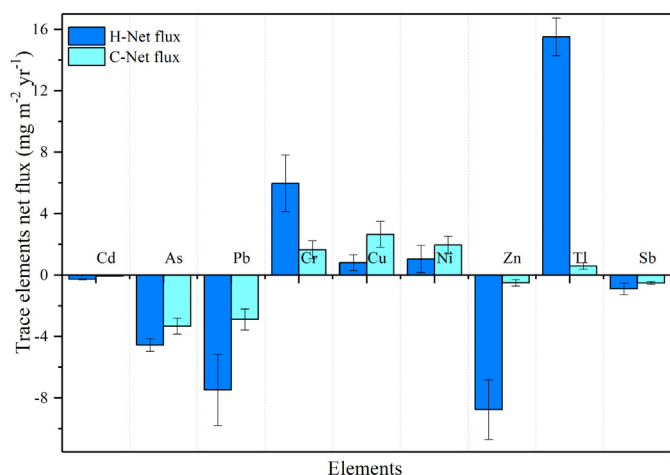


Fig. 5. Schematic illustration of the TEs mass balances in Huilong (denoted as H-) and Chenqi (C-) catchment. The error bars denote the standard deviation (1SD) from the mean. A positive flux indicates a source, and a negative one indicates a sink.

4.2. The dominate pathways for TEs mass balance

The contributions of the five input pathways, i.e., fertilization, TSP, litterfall, throughfall, and open field precipitation, are shown in Fig. 6. Litterfall and throughfall were the two dominate input flux pathways for most of the TEs. Throughfall contributed most among the five pathways for As, Cr, and Sb in both Huilong and Chenqi catchments, and it was also a major pathway for Pb in Huilong and Cd, Ni, Zn, and Tl in Chenqi. Litterfall was the primary pathway for Cu in both catchments. TSP contributed least (<7%) for most TEs except Pb and Tl. The input flux of some TEs (e.g., As and Cu) through fertilizers (the second largest pathway) accounts for up to more than 20%. The TE input fluxes from fertilization should not be underestimated either. The impact of fertilization on the TEs inputs in farmland-forestland karst ecosystems requires attention.

The dominant roles that litterfall and throughfall played in the input fluxes of TEs suggest that forest vegetation cover plays an important role in the fate of TEs in these karst areas. The surface soil of the forest floor is rich in organic matter because of the degradation of leaves litter (Rocha Jr et al., 2013; Wei et al., 2020). Chemical processes such as chelation involving TEs greatly reduce the mobility of the TEs input by rainfall and litterfall (Uchimiyi and Bannon, 2013; Weng et al., 2002), which in turn reduces their spread. In the karst areas with high geological background TEs concentrations, the implementation of measures for returning farmland to forests should first focus on sloping farmland, which suffers from severe water and soil erosion, in order to effectively alleviate the spread of TEs to wider areas.

The crops harvest was the dominant TE output flux pathway in Huilong and Chenqi catchments (Fig. 7). The crops harvest accounted for more than 50% of the total output fluxes of Cr, Cu, Ni, Zn, and Tl in Huilong catchment and more than 93% of the total output fluxes of Cd, Cr, Cu, Ni, Zn, and Tl in Chenqi catchment. Thus, the impact of crops harvest on TEs mass balance in the farmland-forestland compound ecosystems and TEs exposure risks of residents through the consumption of local agricultural products need to be accurately assessed. The relative contributions from different output pathways to the total output flux varied with element because (1) different crops have different absorption and accumulation capabilities of the same TE, and (2) the same crop has different absorption and accumulation capabilities of different elements (Antoniadis et al., 2017; Mwesigye et al., 2019; You et al., 2020). For example, cabbage was a hyperaccumulator of soil Tl (Ning et al., 2015), and cabbage was the main crop planted in Huilong catchment, which resulted in particularly high proportion (99%) of Tl removed by crops harvest.

The implementation of ecological restoration projects will help alleviate soil erosion and increase farmers' income (Li et al., 2016; Tang et al., 2019). Based on the results of this study, in fragile karst areas with high geological background TEs, forest restoration from low-yield sloping farmlands will increase the influx of potentially harmful TEs through litterfall and throughfall and will reduce their output through crop harvesting, which in turn will effectively reduce the disorderly spread of TEs to the surrounding environment.

The quantitative results on TEs input and output flux pathways presented above certainly have some uncertainties caused by many different factors, e.g., theoretical assumption made in the mass balance equation, precision in experimental and chemical analysis. Besides, the field sampling was conducted only in one hydrologic year, only cover several major crops, and with limited number of samples from each media. Meteorological conditions may differ significantly from year to year, which would impact the mass budget in several environmental media. Nevertheless, these results demonstrated the impact of land use structure on the fate of the TEs in the karst ecosystem, especially the role forests played on preventing TEs from wide spread (Fig. 6).

4.3. Ecological drivers and risks in karst areas with high geological background TEs

The biogeochemical cycle of TEs in karst catchments may be influenced by various ecological drivers, such as vegetation type, soil type, soil organic matter, and the degree of soil erosion (Agnan et al., 2019; Fritsch et al., 2012). The geological background of TEs was one of the most important factors. The geochemical composition of the parent rock provides the basic materials for the development of soil TEs concentrations (Jia et al., 2020; Sahoo et al., 2020). Soil is the central link in the TEs biogeochemical cycle in the karst catchments because TEs in soil are on one hand affected by their dry and wet deposition and runoff, and on the other hand dominated by their migration and transmission intensity in the natural processes occurring in the system.

Results from the present study showed that, at the karst catchment scale, forest vegetation cover can effectively increase the inflow of TEs, and decreasing agricultural activity would significantly reduce the output of TEs. Therefore, in ecologically fragile karst areas with high background levels of harmful TEs, converting sloping farmlands that have experienced serious soil erosion and low agricultural productivity into forestlands, as currently planned in the study region, will effectively reduce the disorderly diffusion of harmful TEs into the surrounding environment, which will in turn reduce the associated environmental risks. Since crops harvest dominates the output of TEs in the karst catchment, agricultural planting structure may also need to be adjusted to minimize the residents' exposure risk of potential harmful TEs. To reach this goal, all of the major crops grown in karst areas with high TEs background concentrations should be investigated for their accumulation capacities of harmful TEs, results from which could then guide farmers to select crops with low accumulation capacities for harmful TEs.

5. Conclusions and implications

The mass balances of nine TEs in two karst catchments in southwest China were quantified by considering TEs concentrations in major input/output flux pathways. Litterfall and throughfall dominated the input flux, while crop harvest dominated the output flux. Zinc was the one with the highest concentration in environmental media, and a few others, such as Cu, As, and Pb, also had very high concentrations. For farmland-forestland karst catchment ecosystems, farming activities such as fertilization and crop harvest exert important influence on the TEs mass balance. Therefore, the land use structure played a vital role in the mass balances of TEs in karst catchments. In order to reduce the disorderly diffusion of potentially harmful TEs to the surrounding environment in karst areas with high geological backgrounds, appropriate

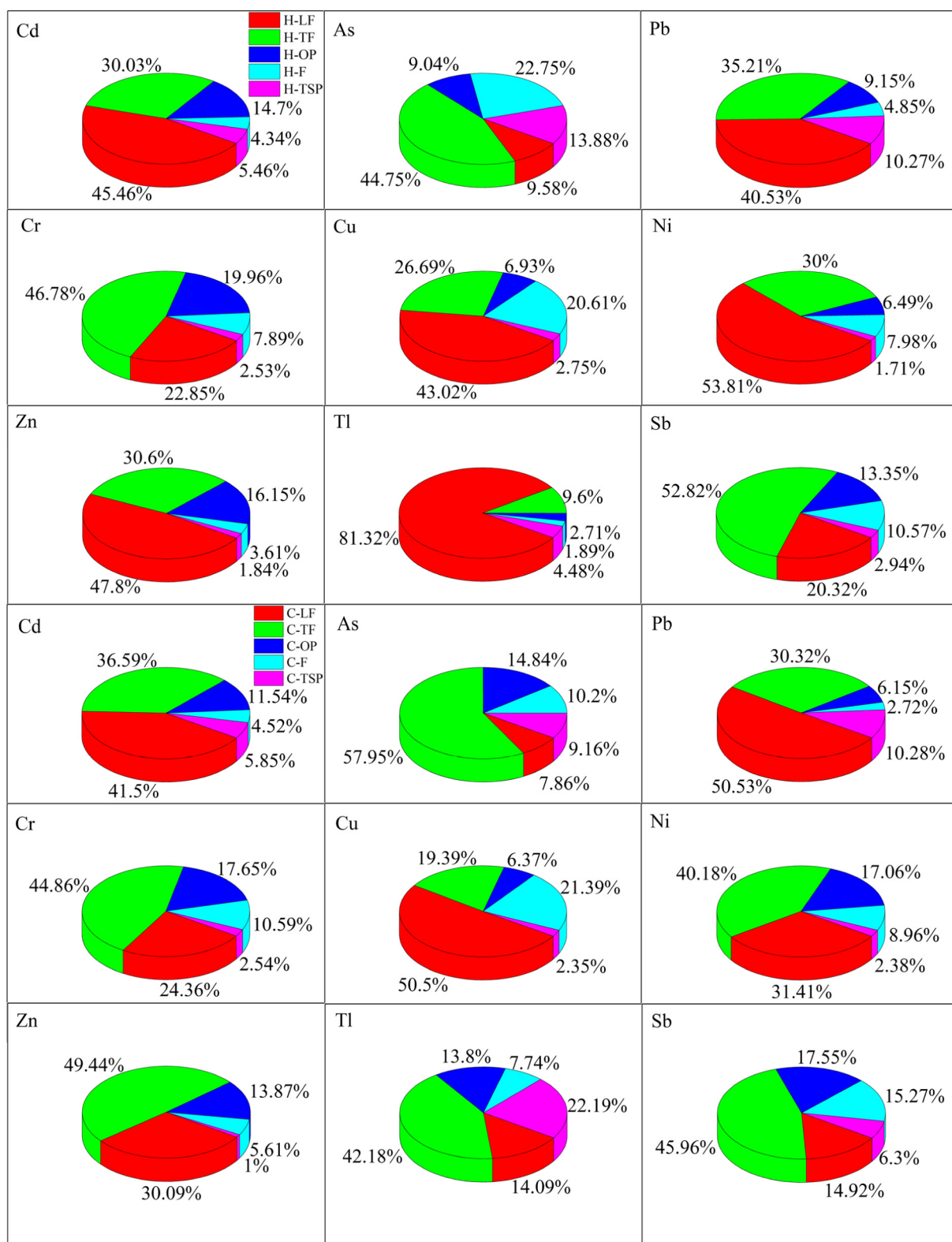


Fig. 6. Relative proportions of the five input flux pathways: litterfall (LF), throughfall (TF), open field precipitation (OP), fertilization (F), and TSP in Huilong (H-LF, H-TF, H-OP, H-F, and H-TSP) and Chenqi (C-LF, C-TF, C-OP, C-F, and C-TSP) catchments.

conversion of farmlands to forests is likely an effective approach, e.g., starting with low yield and high TEs risk farmlands. Future research should focus on the potential environmental impacts of afforestation and should identify the optimum approaches for the conversion of farmland to forests in this and other regions with similar environmental

issues. The effects of soil type, soil organic matter, and the degree of soil erosion on TE geochemical processes in karst areas should be comprehensively and systematically studied in order to deepen our knowledge of the major factors that influence the TEs biogeochemical cycles in karst region.

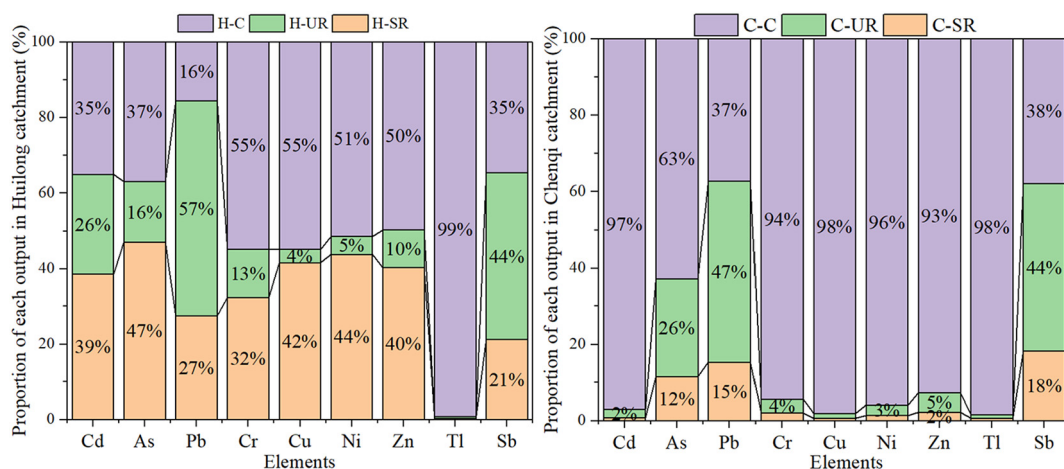


Fig. 7. Proportions of the three output flux pathways: crops harvesting (C), underground runoff (UR), and surface runoff (SR) in Huilong (H-C, H-UR, and H-SR) and Chenqi (C-C, C-UR, and C-SR) catchments.

CRedit authorship contribution statement

Jicheng Xia: Investigation, Methodology, Data curation, Formal analysis, Writing – original draft, Writing – review & editing. **Jianxu Wang:** Supervision, Conceptualization, Writing – review & editing. **Leiming Zhang:** Writing – review & editing, Data curation. **Xun Wang:** Formal analysis, Investigation, Writing – review & editing. **Wei Yuan:** Investigation, Writing – review & editing. **Hui Zhang:** Investigation, Writing – review & editing. **Tao Peng:** Investigation, Data curation. **Xinbin Feng:** Supervision, Conceptualization, Writing – review & editing.

Declaration of competing interest

The authors declare that they have no known competing financial interests or personal relationships that could have appeared to influence the work reported in this paper.

Acknowledgments

This work was supported by the Program Foundation of Institute for Scientific Research of Karst Area of NSFC-GZGOV (U1612442), the National Natural Science Foundation of China (41921004 and 21661132002), the Guizhou Provincial Science and Technology Projects (QKHJC-ZK[2021]YB227), and the Strategic Priority Research Program of Chinese Academy of Sciences (XDB40000000).

Appendix A. Supplementary data

Supplementary data to this article can be found online at <https://doi.org/10.1016/j.scitotenv.2021.147504>.

References

Agnan, Y., Courault, R., Alexis, M.A., Zanardo, T., Cohen, M., Sauvage, M., et al., 2019. Distribution of trace and major elements in subarctic ecosystem soils: sources and influence of vegetation. *Sci. Total Environ.* 682, 650–662.

Aničić, M., Spasić, T., Tomašević, M., Rajšić, S., Tasić, M., 2011. Trace elements accumulation and temporal trends in leaves of urban deciduous trees (*Aesculus hippocastanum* and *Tilia* spp.). *Ecol. Indic.* 11, 824–830.

Antoniadis, V., Levizou, E., Shaheen, S.M., Ok, Y.S., Sebastian, A., Baum, C., et al., 2017. Trace elements in the soil-plant interface: phytoavailability, translocation, and phytoremediation—a review. *Earth-Sci. Rev.* 171, 621–645.

Bi, X.Y., Feng, X.B., Yang, Y.G., Qiu, G.L., Li, G.H., Li, F.L., et al., 2006. Environmental contamination of heavy metals from zinc smelting areas in Hezhang County, Western Guizhou, China. *Environ. Int.* 32, 883–890.

Bini, C., Sartori, G., Wahsha, M., Fontana, S., 2011. Background levels of trace elements and soil geochemistry at regional level in NE Italy. *J. Geochem. Explor.* 109, 125–133.

Bolan, N., Adriano, D., Mahimairaja, S., 2004. Distribution and bioavailability of trace elements in livestock and poultry manure by-products. *CRC Crit. Rev. Environ. Control.* 34, 291–338.

Brinkmann, R., Parise, M., 2012. Karst environments: problems, management, human impacts, and sustainability an introduction to the special issue. *J. Cave Karst Stud.* 74, 135–136.

Cao, Y., Wang, S., Bai, X., Li, H., Zeng, C., Tian, Y., et al., 2018. Estimation of soil erosion considering soil loss tolerance in karst area. *Natural Hazards and Earth System Sciences Discussions*, pp. 1–23.

Censi, P., Cibella, F., Falcone, E.E., Cuttitta, G., Saiano, F., Inguaggiato, C., et al., 2017. Rare earths and trace elements contents in leaves: a new indicator of the composition of atmospheric dust. *Chemosphere* 169, 342–350.

Ci, Z.J., Zhang, X.S., Wang, Z.W., Wang, C.J., 2014. Mass balance of mercury for the yellow sea downwind and downstream of east asia: the preliminary results, uncertainties and future research priorities. *Biogeochemistry* 118, 243–255.

Fajkovic, H., Hasan, O., Miko, S., Juracic, M., Mesic, S., Prohic, E., 2011. Vulnerability of the karst area related to potentially toxic elements. *Geol. Croat.* 64, 41–48.

Feng, X.B., Jiang, H.M., Qiu, G.L., Yan, H.Y., Li, G.H., Li, Z.G., 2009. Mercury mass balance study in wujiangdu and dongfeng reservoirs, Guizhou, China. *Environ. Pollut.* 157, 2594–2603.

Fritsch, C., Coeurdassier, M., Faivre, B., Baurand, P.E., Giraudoux, P., van den Brink, N.W., et al., 2012. Influence of landscape composition and diversity on contaminant flux in terrestrial food webs: a case study of trace metal transfer to european blackbirds *turdus merula*. *Sci. Total Environ.* 432, 275–287.

Gao, N., Armatas, N.G., Shanley, J.B., Kamman, N.C., Miller, E.K., Keeler, G.J., et al., 2006. Mass balance assessment for mercury in lake champlain. *Environ. Sci. Technol.* 40, 82–89.

Gill, L.W., Babechuk, M.G., Kamber, B.S., McCormack, T., Murphy, C., 2018. Use of trace and rare earth elements to quantify autogenic and allogenic inputs within a lowland karst network. *Appl. Geochem.* 90, 101–114.

Huang, Q.H., Cai, Y.L., Xing, X.S., 2008. Rocky desertification, antidesertification, and sustainable development in the karst mountain region of southwest China. *Ambio* 37, 390–392.

Huang, R.J., Cheng, R., Jing, M., Yang, L., Li, Y.J., Chen, Q., et al., 2018. Source-specific health risk analysis on particulate trace elements: coal combustion and traffic emission as major contributors in wintertime Beijing. *Environ. Sci. Technol.* 52, 10967–10974.

Imseng, M., Wiggenshauser, M., Muller, M., Keller, A., Frossard, E., Wilcke, W., et al., 2019. The fate of Zn in agricultural soils: a stable isotope approach to anthropogenic impact, soil formation, and soil-plant cycling. *Environ. Sci. Technol.* 53, 4140–4149.

Jia, Z., Wang, J., Zhou, X., Zhou, Y., Li, Y., Li, B., et al., 2020. Identification of the sources and influencing factors of potentially toxic elements accumulation in the soil from a typical karst region in Guangxi, southwest China. *Environ. Pollut.* 256, 113505.

Jiang, Z.C., Lian, Y.Q., Qin, X.Q., 2014. Rocky desertification in southwest China: impacts, causes, and restoration. *Earth-Sci. Rev.* 132, 1–12.

Li, Q., Liu, Z., Zander, P., Hermanns, T., Wang, J., 2016. Does farmland conversion improve or impair household livelihood in smallholder agriculture system? A case study of grain for green project impacts in China's Loess Plateau. *World Dev. Perspect.* 2, 43–54.

Li, S., Jia, Z., 2018. Heavy metals in soils from a representative rapidly developing megacity (SW China): levels, source identification and apportionment. *Catena* 163, 414–423.

Lin, W.T., Wu, K.M., Lao, Z.L., Hu, W., Lin, B.J., Li, Y.L., et al., 2019. Assessment of trace metal contamination and ecological risk in the forest ecosystem of Dexing Mining Area in Northeast Jiangxi Province, China. *Ecotoxicol. Environ. Safe.* 167, 76–82.

Liu, J., Yin, M., Xiao, T., Zhang, C., Tsang, D.C.W., Bao, Z., et al., 2020. Thallium isotopic fractionation in industrial process of pyrite smelting and environmental implications. *J. Hazard. Mater.* 384, 121378.

Liu, M.D., Zhang, Q.R., Ge, S.D., Mason, R.P., Luo, Y., He, Y.P., et al., 2019. Rapid increase in the lateral transport of trace elements induced by soil erosion in major karst regions in China. *Environ. Sci. Technol.* 53, 4206–4214.

Luo, X.S., Bing, H.J., Luo, Z.X., Wang, Y.J., Jin, L., 2019. Impacts of atmospheric particulate matter pollution on environmental biogeochemistry of trace metals in soil-plant system: a review. *Environ. Pollut.* 255.

- Macleod, M., Mckone, T.E., Mackay, D., 2005. Mass balance for mercury in the San Francisco Bay Area. *Environ. Sci. Technol.* 39, 6721–6729.
- Mamun, A.A., Cheng, I., Zhang, L., Dabek-Zlotorzynska, E., Charland, J.-P., 2019. Overview of size distribution, concentration, and dry deposition of airborne particulate elements measured worldwide. *Environ. Rev.* 1–12.
- Mwesigye, A.R., Young, S.D., Bailey, E.H., Tumwebaze, S.B., 2019. Uptake of trace elements by food crops grown within the Kilembe Copper Mine Catchment, western Uganda. *J. Geochem. Explor.* 207, 106377.
- Ning, Z., He, L., Xiao, T., Marton, L., 2015. High accumulation and subcellular distribution of thallium in green cabbage (*Brassica oleracea* L. var. *capitata* L.). *Int. J. Phytoremed.* 17, 1097–1104.
- Peng, B., Rate, A., Song, Z., Yu, C., Tang, X., Xie, S., et al., 2014. Geochemistry of major and trace elements and pb–sr isotopes of a weathering profile developed on the lower cambrian black shales in central Hunan, China. *Appl. Geochem.* 51, 191–203.
- Rocha Jr., P.R.D., Donagemma, G.K., Andrade, F.V., Passos, R.R., Balieiro, F.D.C., Mendonça, E.D.S., et al., 2013. Can soil organic carbon pools indicate the degradation levels of pastures in the Atlantic forest biome? *J. Agric. Sci.* 6, 84–95.
- Sahoo, P.K., Dall'Agnol, R., Salomão, G.N., Jdsf, Junior, Silva, M.S., e Souza Filho, P.W.M., et al., 2020. Regional-scale mapping for determining geochemical background values in soils of the Itacaiúnas River Basin, Brazil: the use of compositional data analysis (coda). *Geoderma* 376, 114504.
- Su, T.Z., Shu, S., Shi, H.L., Wang, J.M., Adams, C., Witt, E.C., 2008. Distribution of toxic trace elements in soil/sediment in post-Katrina New Orleans and the Louisiana Delta. *Environ. Pollut.* 156, 944–950.
- Sun, J.L., Zou, X., Ning, Z.P., Sun, M., Peng, J.Q., Xiao, T.F., 2012. Culturable microbial groups and thallium-tolerant fungi in soils with high thallium contamination. *Sci. Total Environ.* 441, 258–264.
- Sun, X.X., Li, B.Q., Han, F., Xiao, E.Z., Wang, Q., Xiao, T.F., et al., 2019. Vegetation type impacts microbial interaction with antimony contaminants in a mining-contaminated soil environment. *Environ. Pollut.* 252, 1872–1881.
- Tang, H., Yun, W., Liu, W., Sang, L., 2019. Structural changes in the development of china's farmland consolidation in 1998–2017: changing ideas and future framework. *Land Use Policy* 89, 104212.
- Uchimiya, M., Bannon, D.I., 2013. Solubility of lead and copper in biochar-amended small arms range soils: influence of soil organic carbon and ph. *J. Agric. Food Chem.* 61, 7679–7688.
- Wei, X., Yang, Y., Shen, Y., Chen, Z., Dong, Y., Wu, F., et al., 2020. Effects of litterfall on the accumulation of extracted soil humic substances in subalpine forests. *Front. Plant Sci.* 11.
- Weiss, D., Shoty, W., Riele, J., Page, S., Gloor, M., Reese, S., et al., 2002. The geochemistry of major and selected trace elements in a forested peat bog, Kalimantan, SE Asia, and its implications for past atmospheric dust deposition. *Geochim Cosmochim Acta* 66, 2307–2323.
- Weng, L.P., Temminghoff, E.J.M., Lofts, S., Tipping, E., Van Riemsdijk, W.H., 2002. Complexation with dissolved organic matter and solubility control of heavy metals in a sandy soil. *Environ. Sci. Technol.* 36, 4804–4810.
- Wu, W., Qu, S., Nel, W., Ji, J., 2020. The impact of natural weathering and mining on heavy metal accumulation in the karst areas of the Pearl River Basin, China. *Sci. Total Environ.* 734, 139480.
- Xia, J., Wang, J., Zhang, L., Wang, X., Yuan, W., Anderson, C.W.N., et al., 2021. Significant mercury efflux from a karst region in southwest China — results from mass balance studies in two catchments. *Sci. Total Environ.* 769, 144892.
- Xia, Longlong, Shu, Kee, La, Xiaoyuan, et al., 2017. How does recycling of livestock manure in agroecosystems affect crop productivity, reactive nitrogen losses, and soil carbon balance? *Environ. Sci. Technol.* 51, 7450–7457.
- Xiao, E.Z., Ning, A.P., Xiao, T.F., Sun, W.M., Qiu, Y.Q., Zhang, Y., et al., 2019. Variation in rhizosphere microbiota correlates with edaphic factor in an abandoned antimony tailing dump. *Environ. Pollut.* 253, 141–151.
- Xiao, Guha J., Boyle, D., C-Q, Liu, Chen, J., 2004a. Environmental concerns related to high thallium levels in soils and thallium uptake by plants in southwest Guizhou, China. *Sci. Total Environ.* 318, 223–244.
- Xiao, T., Guha, J., Boyle, D., Liu, C.Q., Zheng, B., Wilson, G.C., et al., 2004b. Naturally occurring thallium: a hidden geoenvironmental health hazard? *Environ. Int.* 30, 501–507.
- You, R., Margenat, A., Lanzas, C.S., Canameras, N., Carazo, N., Navarro-Martin, L., et al., 2020. Dose effect of zn and cu in sludge-amended soils on vegetable uptake of trace elements, antibiotics, and antibiotic resistance genes: human health implications. *Environ. Res.* 191, 109879.
- Zhao, M., Zeng, C., Liu, Z., Wang, S., 2010. Effect of different land use/land cover on karst hydrogeochemistry: a paired catchment study of Chenqi and Dengzhanhe, Puding, Guizhou, SW China. *J. Hydrol.* 388, 121–130.
- Zheng, J.C., Shoty, W., Krachler, M., Fisher, D.A., 2007. A 15,800-year record of atmospheric lead deposition on the Devon Island Ice Cap, Nunavut, Canada: natural and anthropogenic enrichments, isotopic composition, and predominant sources. *Global Biogeochem Cy* 21, 20–22.